ACS chemical biology

Letters

pubs.acs.org/acschemicalbiology

Electrostatically Controlled Quantum Dot Monofunctionalization for Interrogating the Dynamics of Protein Complexes in Living Cells

Changjiang You,* Stephan Wilmes, Christian P. Richter, Oliver Beutel, Domenik Liße, and Jacob Piehler*

Division of Biophysics, Department of Biology, University of Osnabrück, 49076 Osnabrück, Germany

Supporting Information

ABSTRACT: Quantum dots (QD) are powerful labels for probing diffusion and interaction dynamics of proteins on the single molecule level in living cells. Protein cross-linking due to multifunctional QD strongly affects these properties. This becomes particularly critical when labeling interaction partners with QDs for interrogating the dynamics of complexes. We have here implemented a generic method for QD monofunctionalization based on electrostatic repulsion of a highly negatively charged peptide carrier. On the basis of this method, monobiotinylated QDs were prepared with high yield as confirmed by single molecule assays. These QDs were successfully employed for probing the assembly and diffusion dynamics of binary and ternary cytokine−receptor complexes on the surface of living cells by dual color single QD tracking. Thus, sequential and dynamic recruitment of the type I interferon receptor subunits by the ligand could be observed.

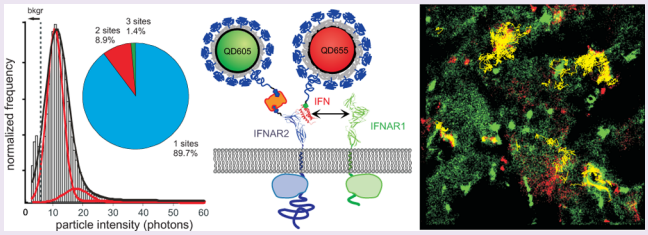

Transport and communication across the plasma membrane require the assembly of membrane proteins into functional entities. Submicroscopic compartmentation caused by an interplay of the cortical actin skeleton, lipid phase separation, and protein−protein interactions have been shown to result into a complex and highly dynamic lateral organization of proteins within the plasma membrane of mammalian cells.[1−3] Single molecule imaging techniques have contributed tremendously to unraveling the dynamic organization of proteins and lipids in the plasma membrane as they allow tracking the motion of individual proteins with very high spatial and temporal resolution.[3−6] However, exploring the contribution of protein−protein interactions to membrane microcompartmentation requires tools for reliably identifying and tracking individual membrane protein complexes. Owing to their high brightness and photostability, quantum dots (QD) and other fluorescent nanoparticles are frequently used for labeling of proteins and lipids, thus enabling to follow individual species in living cells over extended time periods.[7−16] While tracking of cell surface proteins labeled with QDs is well established, only very few successful studies have been reported, which involve systematic interrogation of protein complex formation.[3,17] Conjugation of target proteins with QDs in a 1:1 stoichiometry is an important prerequisite in order to ensure minimum bias of diffusion and interaction dynamics. This is particularly critical for probing protein complexes with both interaction partners labeled by a QD. In this case, the interaction dynamics could be affected by multivalent binding and ultimately could induce particle aggregation. Moreover, efficient QD conjugation to target proteins on the cell surface is required for achieving a high degree of labeling with minimum non-specific background in order to ensure a significant probability that both interaction partners within a complex carry a QD. While various selective and orthogonal functionalization strategies for nanoparticle targeting have been reported,[9,12,18−25] control of the degree of functionalization remains challenging and often requires demanding purification methods.[26−28] For this purpose, gel electrophoresis and anion exchange and affinity chromatography have been successfully applied.[26,28−32] These techniques, however, require relatively small and highly monodisperse QDs, while surface coatings providing good biocompatibility often render QD relatively large with a rather heterogeneous distribution of sizes and charges. Moreover, statistic functionalization followed by purification not only increases complexity of the procedure but also reduces the overall yield.

We have recently observed that the reaction of maleimide-functionalized QDs with a thiol-functionalized tris-nitrilotriacetic acid (tris-NTA) moiety could be tuned toward a 1:1 functionalization ratio by coupling at low ionic strength at neutral pH.[33] Under these conditions, tris-NTA has a net charge of −6. We attributed QD monofunctionalization to a reduction of the reaction rate constant due to the increase in electrostatic repulsion upon coupling of the first tris-NTA moiety. Thus, reaction with a nonfunctionalized QD is more probable than with a QD carrying a tris-NTA moiety, steering the reaction toward monofunctionalization. Here, we have explored direct QD monofunctionalization by coupling negatively charged peptides carrying a biotin moiety. The rapid, quasi-irreversible interaction of biotin-streptavidin is ideally suitable for probing the degree of functionalization on

Received: October 5, 2012
Accepted: November 27, 2012
Published: November 27, 2012

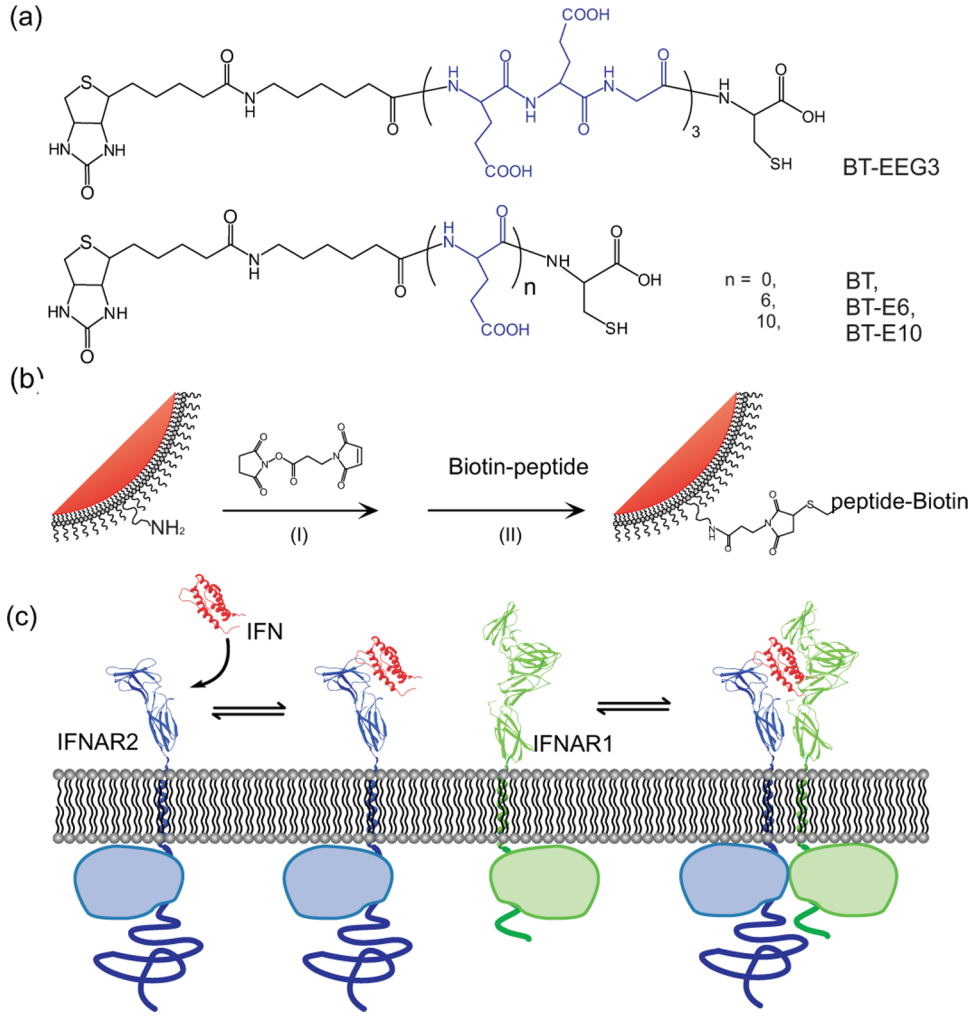

Figure 1. (a,b) QD functionalization controlled by electrostatic repulsion. (a) Biotinylated peptides used for QD functionalization. (b) Coupling reaction on the surface of commercially available QDs functionalized with amine groups. After reaction with the heterobifunctional crosslinker maleimidopropionic acid-*N*-hydroxysuccinimide (I), biotinylated peptides were coupled through their cysteine residues (II). (c) Two-step assembly of the type I interferon receptor complex as suggested by *in vitro* studies.[39]

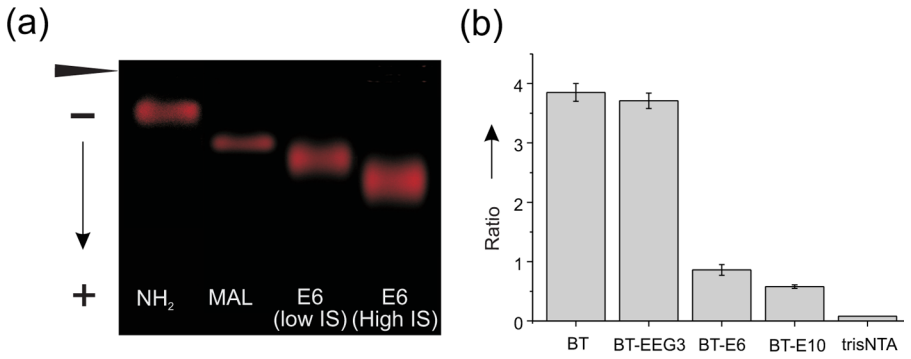

Figure 2. Ensemble characterization of biotin peptide functionalized QDs. (a) Agarose gel electrophoresis of QDs before functionalization (NH_2), after reaction with maleimidopropionic acid-*N*-hydroxysuccinimide (Mal), and after coupling of BT-E6 at low and at high ionic strength (IS), respectively. (b) Average number of streptavidin binding sites determined by analytical SEC.

the single particle level and moreover ensures efficient protein labeling on the cell surface as required for probing interactions on level of individual complexes. Different peptide sequences were tested, varying in the number (6 and 10 glutamic acid residues) as well as the density of negative charges, and compared to a noncharged, biotinylated control peptide (Figure 1a). By means of a cysteine residue, these peptides were coupled to commercially available, polymer-coated QD functionalized with amine groups (~30−40/QD) *via* maleimidopropionic acid-*N*-hydroxysuccinimide as a heterobifunctional cross-linker (Figure 1b). These QDs have a diameter of ~23 nm with a relatively broad distribution.[33] The degree of QD functionalization was characterized in detail, and monofunctionalized QD were used for labeling site-specifically

dx.doi.org/10.1021/cb300543t | *ACS Chem. Biol.* 2013, 8, 320−326

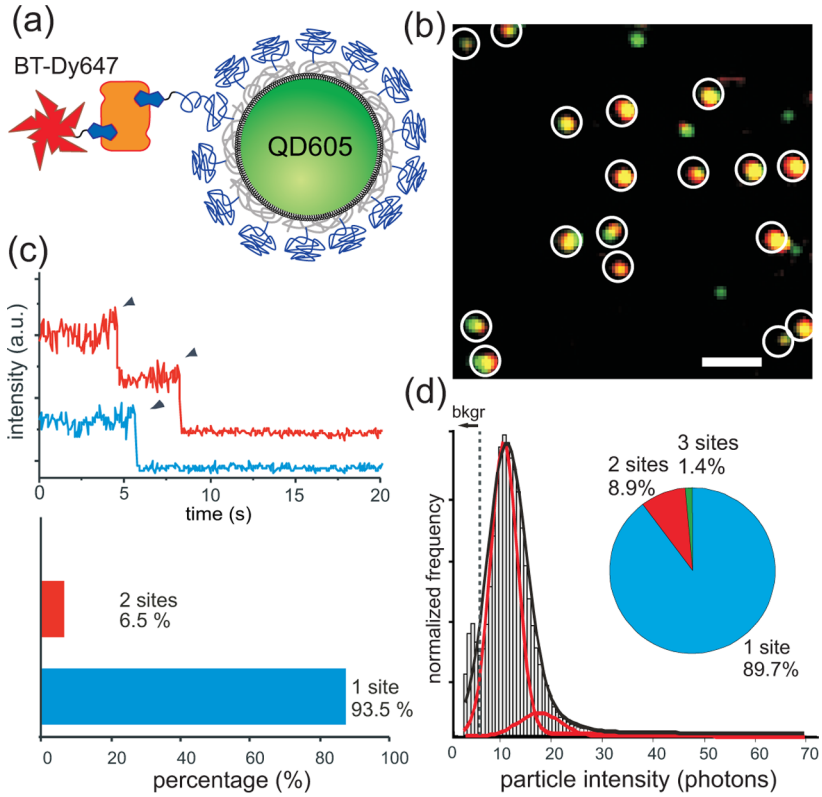

Figure 3. Stoichiometry of biotin functionalization probed by single molecule imaging. (a) Conjugation of biotin-functionalized QD with BT-Dy647 *via* bSAV. (b) Merged TIRFM image of $^{BT\text{-}E6}$QD605 (green) and BT-Dy647 (red). White circles highlight co-localized signals from both channels (scale bar: 2 μm). (c) Photobleaching step-counting analysis of co-localized spots in the Dy647 channel for $^{BT\text{-}E6}$QD605-bSAV/BT-Dy647 complex obtained from 127 traces. (d) Particle intensity histogram analysis of individual particles detected in the Dy647 channel from the $^{BT\text{-}E6}$QD605-bSAV/BT-Dy647 complex.

biotinylated proteins on the cell surface in a 1:1 stoichiometry *via* bifunctional streptavidin (bSAV)[27] for probing the dynamics of type I interferon (IFN) receptor assembly in the plasma membrane (Figure 1c).

QD functionalization was monitored by gel electrophoresis (Figure 2a and Supplementary Figure 1). For all negatively charged peptides, a small shift in the electrophoretic mobility was observed upon coupling at low ionic strength, which was much stronger upon coupling at high ionic strength. These results supported our hypothesis that electrostatic repulsion can control the degree of QD functionalization. The average number of biotin moieties on QDs was quantified by analytical size exclusion chromatography (SEC). To this end, functionalized QD605 (10 nM) were incubated with a large excess (500 nM) of monovalent streptavidin[34] labeled with ATTO647N (^{AT647N}mSAV). Co-elution of ^{AT647N}mSAV with QD605 functionalized with biotinylated peptides was observed (Supplementary Figure 2). In contrast, QD605 functionalized with tris-NTA showed negligible binding of ^{AT647N}mSAV, confirming specific ^{AT647N}mSAV capturing by biotin moieties on the QD surface. The ^{AT647N}mSAV:QD605 ratio was calculated from the peak signals at 350 nm (QD605) and 650 nm (^{AT647N}mSAV) (Figure 2b). For BT-E6 coupled at low ionic strength, an average number of 0.86 ± 0.08 streptavidin binding sites per QD was determined, corroborating self-controlled monofunctionalization of a highly negatively charged ligand. For BT-E10, an even lower number of streptavidin binding sites per QD was observed under these coupling conditions. Thus, 10 negative charges seem to reduce the reaction rate constant to a level at which coupling to nonfunctionalized QD (which are also slightly negatively charged) is no longer efficient. In contrast, the peptide BT-EEG3 yielded a similar number of streptavidin binding sites as the control peptide, suggesting a critical role of charge density for controlling nanoparticle functionalization by electrostatic steering.

Functionalization of QD with biotin was further characterized by real-time solid phase binding assays using reflectance interference detection. To this end, His-tagged bSAV[34] was immobilized on a poly(ethylene glycol) (PEG) polymer brush surface functionalized with tris-NTA, which was loaded with Ni(II) ions.[35,36] A typical binding assays including streptavidin immobilization, QD binding and elution with imidazole is shown in Supplementary Figure 3. Specific binding of QDs functionalized with BT-E6 to immobilized streptavidin was observed (Supplementary Figure 3b). QDs functionalized with BT-EEG3 showed faster binding and a lower binding amplitude, which can be explained by their higher degree of functionalization. Multivalent binding was probed by monitoring the dissociation kinetics during injection of imidazole (Supplementary Figure 3c). Strikingly, the dissociation kinetics of BT-E6-functionalized QD (0.11 ± 0.02 s^{-1}) was only slightly decreased compared to the dissociation kinetics of streptavidin alone (0.14 ± 0.02 s^{-1}). In contrast, significantly slower dissociation was observed for BT-EEG3-functionalized QD (0.065 ± 0.01 s^{-1}). This decreased rate constant can be explained by cross-linking of two or more streptavidin molecules, which are immobilized on the surface with very high density (~50% of a monolayer). Thus, these binding

dx.doi.org/10.1021/cb300543t | *ACS Chem. Biol.* 2013, 8, 320–326

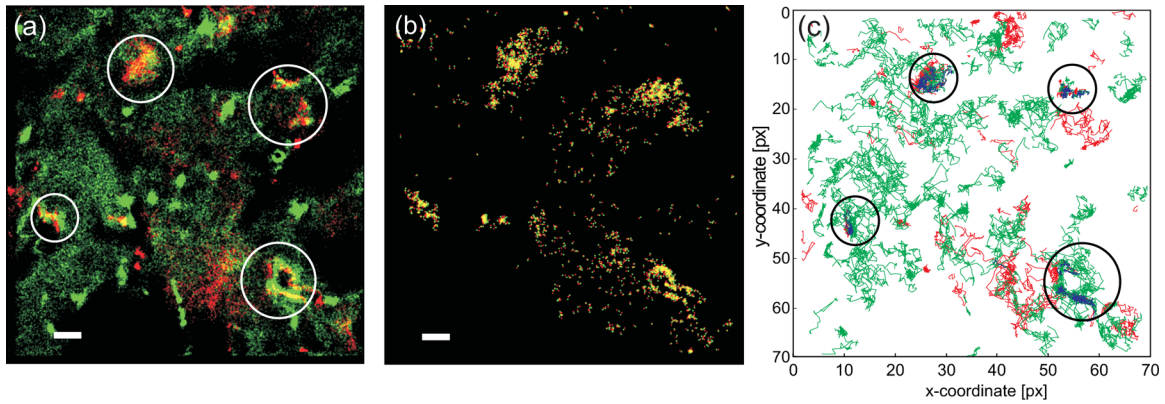

Figure 4. Co-localization and co-locomotion analysis for IFNα2 labeled with QD655 (red) bound to AP-IFNAR2 labeled with QD605 (green). (a) TALM image rendered from individual QD655 and QD605 localized within 1000 consecutive frames. (b) Same ROI after filtering for co-localization of QD655 and QD605 within 50 nm in each frame. Scale bar: 500 nm. (c) Trajectories obtained by tracking of QD655 (red), QD605 (green), and QD655/QD605 co-localized within 100 nm for more than 15 consecutive steps (blue). The circles mark regions where individual complexes were detected.

experiments confirmed that QD functionalized with BT-E6 were mostly monofunctional.

These binding assays, however, probed the average degree of functionalization within the ensemble and thus did not provide detailed information how the biotin moieties were distributed on the single QD level. We employed single molecule imaging for determining the stoichiometry of streptavidin binding on individual QDs.[27] For this purpose, $^{BT\text{-}E6}$QD605 was reacted with bSAV, which was prepared without a His-tag[27,34] in order to avoid direct binding to the QD surface. Subsequently, the free biotin binding sites of the surface-bound streptavidin were reacted with biotinylated Dy647 (BT-Dy647, Figure 3a).

After purification by SEC (Supplementary Figure 4), these QDs were adsorbed onto the surface of a coverslip, and the fluorescence from the QD and the attached dye was recorded by time-lapse dual color single molecule imaging. A typical image from such an experiment is shown in Figure 3b. The true QD−protein complexes were rigorously discriminated from randomly co-localized pairs by analysis co-localization beyond the diffraction limit (Supplementary Figure 5). This analysis revealed that ~80% of the $^{BT\text{-}E6}$QD605 co-localized with BT-Dy647 with a proximity of <50 nm, confirming a high degree of QD functionalization on the single particle level. The number of BT-Dy647 bound to $^{BT\text{-}E6}$QD605 was evaluated by a fluorescence intensity distribution analysis (Figure 3d). Strikingly, this analysis revealed that 90% of the QD were monofunctional. We also analyzed the stoichiometry by photobleaching the attached Dy647 (Figure 3c),[27] which corroborated monofunctionalization of >90%. Using commercial SAv instead of bSAv in theses assays yielded a distribution of 1−3 biotin binding sites (Supplementary Figure 6), thus confirming a high degree of monobiotinylation. These analyses clearly demonstrate that coupling under conditions of strong electrostatic repulsion not only yields a low average functionalization but also efficiently steers the stoichiometry toward QD monofunctionalization. Taking into account losses during preparation (~60%), the overall yield of monofunctional QD was ~34%.

We employed these monobiotinylated QDs for exploring assembly and dynamics of protein complexes on the surface of living cells. As a model system, the interaction of the type I interferon (IFN) receptor subunits IFNAR1 and IFNAR2 with its ligand IFNα2 was employed. IFNα2 binds IFNAR2 with a K_D of ~5 nM, while its binding affinity toward IFNAR1 is ~1000-fold lower.[36] For probing complex formation between IFNα2 and IFNAR2 on the cell surface, we generated HeLa cells stably expressing IFNAR2 fused to an N-terminal acceptor peptide (AP) tag for enzymatic biotinylation.[10] These cells express IFNAR2 at a cell surface concentration of ~2 molecules/μm^2 as determined by binding of dye-labeled IFNα2 (Supporting Methods). This cell surface concentration is only slightly above the physiological expression level (0.1−1 molecules/μm^2).[37] Binding of $^{BT\text{-}E6}$QD605 to these cells was observed only after biotinylation and binding of bSAV (Videos 1 and 2 in Supporting Information, Supplementary Figure 7), confirming the specificity of labeling in living cells. A similar degree of cell surface labeling was observed compared to labeling with ^{AT647N}mSAV (Video 3 in Supporting Information). By comparison with dye-labeled IFNα2 binding, labeling of ~30% of cell surface IFNAR2 was estimated. IFNα2 fused to an N-terminal His-tag was labeled with monofunctional $^{tris\text{-}NTA}$QD655 as described before.[33] These have been previously shown to bind highly specifically to cells expressing IFNAR2.[33] Binding of QD655-labeled IFNα2 (IFNα2-QD655) to IFNAR2 labeled with QD605 was monitored by dual-color time-lapse experiments (Video 4 in Supporting Information) and analyzed by tracking and localization microscopy (TALM)[38] (Figure 4a). For both channels, localization of individual QD was possible with a localization precision <25 nm (Supplementary Figure 8). By comparison with the IFNAR2 expression level of these cells (see above) an overall fraction of ~30% occupancy with QD655-labeled IFNα2 was estimated. Co-localization of QD605 and QD655 was detectable at several sites in the obtained super-resolution image, indicating complex formation between QD605-labeled IFNAR2 and QD655-labeled IFNα2 (Figure 4a,b). Formation of such complexes was confirmed by co-locomotion analysis (Video 5 in Supporting Information and Figure 4c), which was analyzed by tracking co-localized molecules over multiple frames. Thus, randomly co-localized QDs are eliminated as these are not spatially correlated over multiple frames. The fraction of complexes obtained after filtering for co-locomotion of at least 6 frames was 8.0 ± 1%, which is close to the 9% as expected for a labeling degree of 30% for both interaction partners.

dx.doi.org/10.1021/cb300543t | ACS Chem. Biol. 2013, 8, 320−326

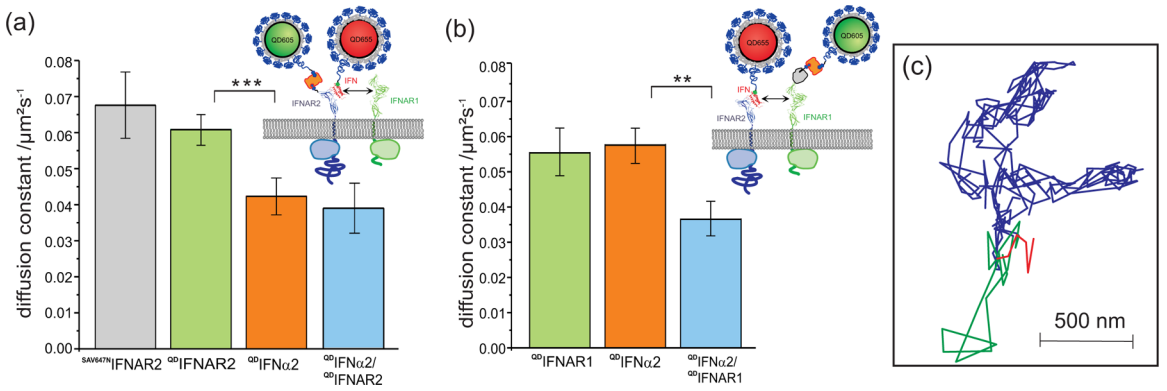

Figure 5. Dynamics of individual protein complexes in the plasma membrane of living cells. (a) Diffusion constants of IFNAR2/$^{BT\text{-}E6}$QD605 (green), IFNα2/$^{tris\text{-}NTA}$QD655 (red) bound to the cell surface receptor and the IFNα2/IFNAR2 complex (blue) identified by cotracking (N = 18, ***$P < 10^{-4}$). For comparison, the diffusion constant obtained for IFNAR2 labeled *via* monofunctional streptavidin is shown (gray). (b) Diffusion constants of IFNAR1 labeled with $^{BT\text{-}E6}$QD605 (green), IFNα2 labeled with $^{tris\text{-}NTA}$QD655 (red), and their complex (blue) as identified by cotracking (N = 12, **$P < 10^{-2}$). (c) Tracking of IFNAR2-bound IFNα2/ $^{tris\text{-}NTA}$QD655 interacting with IFNAR1/$^{BT\text{-}E6}$QD605 reveals dissociation of the ternary complex in plane of the membrane (IFNAR1, green; IFNα2, red; cotrajectory, blue).

As all nucleated human cells, HeLa cells express endogenous IFNAR1 and IFNAR2. Thus, ternary complex assembly is possible by simultaneous interaction of IFNα2 with IFNAR1 and IFNAR2. We have previously demonstrated *in vitro* that QD-labeling of IFNα2 still allows efficient ternary complex assembly.[33] In order to further explore the mechanism of IFN-receptor complex formation in living cells, we analyzed the diffusion of different species on the plasma membrane by the step-length analysis method (Supporting method and Supplementary Figure 9). The diffusion constants obtained for the fast mobile fraction are compared in Figure 5a. For QD605-labeled IFNAR2, a diffusion constant of 0.061 ± 0.004 $\mu m^2\ s^{-1}$ was found, which is very similar to the diffusion constant observed for IFNAR2 labeled with ^{AT647N}mSAV. This result confirms that labeling with monofunctional QD does not significantly alter the diffusion properties of a cell surface protein. Strikingly, a significantly lower diffusion rate constant was observed for IFNα2-QD655 bound to the cell surface (0.042 ± 0.005 $\mu m^2\ s^{-1}$). The diffusion constant of IFNα2-QD655 co-locomoting with IFNAR2 yielded the same diffusion constant. These results suggest that IFNα2 binding reduces the diffusion constant of IFNAR2, probably due to ternary complex formation by simultaneous interaction with endogenous IFNAR1.

We therefore further explored ternary complex formation with a cell line stably expressing IFNAR1 fused to an N-terminal HaloTag, which was employed for site-specific biotinylation. After labeling of biotinylated cell surface IFNAR1 with $^{BT\text{-}E6}$QD605 *via* bSAV (Video 6), the interaction with IFNα2-QD655 was probed by dual-color QD imaging. Formation of ternary complexes was revealed by co-locomotion analysis (Video 7). The diffusion constant of 0.038 ± 0.005 $\mu m^2/s$ obtained from the co-locomotion trajectories (Figure 5b) was in good agreement to the reduced diffusion constant observed for IFNα2-QD655 bound to IFNAR2, corroborating that indeed ternary complex formation was responsible for the reduced diffusion constant. Slower diffusion of ternary complexes could be explained either by the increase in friction within the membrane due to cross-linking of the two transmembrane receptor subunits, or by additional interactions of the activated signaling complex. Interestingly, for IFNα2-QD655 only, a similar diffusion constant (0.059 ± 0.005 $\mu m^2\ s^{-1}$) was observed as for free IFNAR1 (0.056 ± 0.007 $\mu m^2 s^{-1}$) and IFNAR2 (see above). We also noticed a significant lower fraction of co-locomotion events (3.2 ± 0.8%) compared to the interaction between IFNα2 and IFNAR2. This result suggests that the efficiency of ternary complex assembly is reduced when simultaneously labeling IFNAR1 with QD and IFNAR2 with IFNα2-QD. This could be ascribed to a reduction in the binding affinity of IFNAR1 toward the IFNα2/IFNAR2 complex due to steric hindrance by QD labeling. Such further reduced binding affinity of this low-affinity interaction could shift the equilibrium between binary and ternary complexes. Taken together, these observations support a dynamic 2-step assembly of the ternary signaling complex as depicted in Figure 1, which may have important implications for regulating signaling specificity.[40] Indeed, by following individual complexes over extended time periods, dissociation of individual complexes could be observed (Figure 5c and Video 8 in Supporting Information). Further studies of the dynamic equilibrium between binary and ternary complexes by co-locomotion analysis can be envisaged yet require orthogonal labeling of both receptor subunits.

In conclusion, we have implemented a generic method for QD monofunctionalization, which is based on controlling the reaction rates by electrostatic repulsion of a negatively charged carrier peptide. Single molecule assays established for the first time that monofunctionalization under these conditions was achieved directly, *i.e.*, without the need for further purification. Systematic variation of the electrostatic properties of the carrier peptide and the coupling conditions corroborated the key role of the number and the density of charges for controlling reactivity. Since the carrier peptide can be functionalized with other biochemical substrates for specific protein targeting, this approach can be readily extended for orthogonal cell surface labeling. A high degree of protein labeling was achieved with these QDs on the surface of living cells, which is of critical importance for visualizing and analyzing protein−protein interactions on the single molecule level. These QDs proved to be suitable for interrogating diffusion and interaction dynamics of ligand−receptor complexes in the plasma membrane of living cells.

METHODS

Procedures for QD monofunctionalization and characterization are provided in the Supporting Information.

dx.doi.org/10.1021/cb300543t | *ACS Chem. Biol.* 2013, 8, 320−326

Protein Labeling with Monofunctional QDs. Site-specific biotinylation of AP-tagged cell surface protein was carried out according to literature procedure.[10] Site-specific biotinylation of Halo-tagged cell surface protein was carried out according to manufacturer's instruction (Promega). After surface protein biotinylation, the cells were incubated with 500 nM His-tag free bSAV[27] at RT for 10 min, followed by washing three times with PBS-BSA. Subsequently, 20 nM $^{BT\text{-}E6}$QD605 in PBS-BSA was added and incubated for 10 min. The cells were then washed with MEM medium containing 10% FBS for three times. Immediately after the $^{BT\text{-}E6}$QD605 labeling, 20 nM IFNα2 freshly labeled with ^{TrisNTA}QD655 was added and incubated for 20 min. The cell sample was then washed three times with medium to remove unbound QDs before imaging experiments. Labeling specificity was confirmed by binding of $^{BT\text{-}E6}$QD605 to biotinylated AP-IFNAR2 without prior incubation of bSAV. The cell was incubated with IFNα2-QD655 as a positive control for AP-IFNAR2 expression and cell surface accessibility.

Dual-Color Single QD Tracking. Single molecule imaging in a TIRFM was carried out with the same setup used for single molecule binding experiments. However, both QD605 and QD655 were excited with the 488 nm laser, and the fluorescence from both channels was collected simultaneously on the same camera chip by means of an image splitter (Dual View, Photometrics). Typical time series of 1000−20,000 frames were recorded at 30 Hz. In order to reduce photooxidation of QDs, an oxygen scavenging system containing 0.5 mg mL^{-1} glucose oxidase, 40 mg mL^{-1} catalase, and 5% w/v glucose was added. Under these conditions, no significant photooxidation of QD was observed within the experiment time (~10 min of continuous illumination). For all dual-color single molecule fluorescence imaging, channels was calibrated by imaging fluorescent microbeads (TetraSpeck microspheres 0.1 μm, T7279, Invitrogen), which was used for calculating a transformation matrix. After channel alignment based on the transformation matrix, the deviation between the channels was below 15 nm.

■ ASSOCIATED CONTENT

Supporting Information

Detailed experimental procedures, supplementary figures and videos. This material is available free of charge *via* the Internet at http://pubs.acs.org.

■ AUTHOR INFORMATION

Corresponding Author

*E-mail: piehler@uos.de; you@biologie.uni-osnabrueck.de.

Notes

The authors declare no competing financial interest.

■ ACKNOWLEDGMENTS

We thank G. Hikade and H. Kenneweg for technical support. Plasmids for producing mSAV and bSAV as well as BirA were kindly provided by A. Ting, MIT. This work was supported by the DFG (PI405-6 and SFB 944) and the European Community's Seventh Framework Programme (FP7/2007-2013) under grant agreement no. 223608 (IFNaction).

■ ABBREVIATIONS

AT647N, ATTO647N dye; AP tag, acceptor peptide tag for biotinylation; BT, biotin; BT-Dy647, biotinylated Dy647 dye; BT-EEG3, Biotin-EEGEEGEEG-C; BT-E6, Biotin-EEEEEE-C; BT-E10, Biotin-EEEEEEEEEE-C; bSAV, bifunctional streptavidin; IFN, interferon; IFNAR1 and IFNAR2, type I interferon receptor subunit 1 and 2; mSAV, monovalent streptavidin; QD, quantum dot; SEC, size exclusion chromatography; tris-NTA, tris-nitrilotriacetic acid; TALM, tracking and localization microscopy; TIRFM, total internal reflection fluorescence microscopy

■ REFERENCES

(1) Marguet, D., Lenne, P. F., Rigneault, H., and He, H. T. (2006) Dynamics in the plasma membrane: how to combine fluidity and order. *EMBO J. 25*, 3446−3457.

(2) Kusumi, A., Fujiwara, T. K., Morone, N., Yoshida, K. J., Chadda, R., Xie, M., Kasai, R. S., and Suzuki, K. G. (2012) Membrane mechanisms for signal transduction: The coupling of the meso-scale raft domains to membrane-skeleton-induced compartments and dynamic protein complexes. *Semin. Cell Dev. Biol. 23*, 126−144.

(3) Cambi, A., and Lidke, D. S. (2012) Nanoscale membrane organization: where biochemistry meets advanced microscopy. *ACS Chem. Biol. 7*, 139−149.

(4) Kusumi, A., Shirai, Y. M., Koyama-Honda, I., Suzuki, K. G., and Fujiwara, T. K. (2010) Hierarchical organization of the plasma membrane: Investigations by single-molecule tracking vs. fluorescence correlation spectroscopy. *FEBS Lett. 584*, 1814−1823.

(5) Owen, D. M., Williamson, D., Rentero, C., and Gaus, K. (2009) Quantitative microscopy: protein dynamics and membrane organisation. *Traffic 10*, 962−971.

(6) Lidke, D. S., and Wilson, B. S. (2009) Caught in the act: quantifying protein behaviour in living cells. *Trends Cell. Biol. 19*, 566−574.

(7) Dahan, M., Levi, S., Luccardini, C., Rostaing, P., Riveau, B., and Triller, A. (2003) Diffusion dynamics of glycine receptors revealed by single-quantum dot tracking. *Science 302*, 442−445.

(8) Lidke, D. S., Nagy, P., Heintzmann, R., Arndt-Jovin, D. J., Post, J. N., Grecco, H. E., Jares-Erijman, E. A., and Jovin, T. M. (2004) Quantum dot ligands provide new insights into erbB/HER receptor-mediated signal transduction. *Nat. Biotechnol. 22*, 198−203.

(9) Michalet, X., Pinaud, F. F., Bentolila, L. A., Tsay, J. M., Doose, S., Li, J. J., Sundaresan, G., Wu, A. M., Gambhir, S. S., and Weiss, S. (2005) Quantum dots for live cells, in vivo imaging, and diagnostics. *Science 307*, 538−544.

(10) Howarth, M., Takao, K., Hayashi, Y., and Ting, A. Y. (2005) Targeting quantum dots to surface proteins in living cells with biotin ligase. *Proc. Natl. Acad. Sci. U.S.A. 102*, 7583−7588.

(11) Bouzigues, C., Morel, M., Triller, A., and Dahan, M. (2007) Asymmetric redistribution of GABA receptors during GABA gradient sensing by nerve growth cones analyzed by single quantum dot imaging. *Proc. Natl. Acad. Sci. U.S.A. 104*, 11251−11256.

(12) Chang, Y. P., Pinaud, F., Antelman, J., and Weiss, S. (2008) Tracking bio-molecules in live cells using quantum dots. *J. Biophotonics 1*, 287−298.

(13) Serge, A., Bertaux, N., Rigneault, H., and Marguet, D. (2008) Dynamic multiple-target tracing to probe spatiotemporal cartography of cell membranes. *Nat. Methods 5*, 687−694.

(14) Pinaud, F., Clarke, S., Sittner, A., and Dahan, M. (2010) Probing cellular events, one quantum dot at a time. *Nat. Methods 7*, 275−285.

(15) Bruchez, M. P. (2011) Quantum dots find their stride in single molecule tracking. *Curr. Opin. Chem. Biol. 15*, 775−780.

(16) Itano, M. S., Neumann, A. K., Liu, P., Zhang, F., Gratton, E., Parak, W. J., Thompson, N. L., and Jacobson, K. (2011) DC-SIGN and influenza hemagglutinin dynamics in plasma membrane microdomains are markedly different. *Biophys. J. 100*, 2662−2670.

(17) Low-Nam, S. T., Lidke, K. A., Cutler, P. J., Roovers, R. C., van Bergen en Henegouwen, P. M., Wilson, B. S., and Lidke, D. S. (2011) ErbB1 dimerization is promoted by domain co-confinement and stabilized by ligand binding. *Nat. Struct. Mol. Biol. 18*, 1244−1249.

(18) Kim, S., and Bawendi, M. G. (2003) Oligomeric ligands for luminescent and stable nanocrystal quantum dots. *J. Am. Chem. Soc. 125*, 14652−14653.

(19) Alivisatos, A. P., Gu, W., and Larabell, C. (2005) Quantum dots as cellular probes. *Annu. Rev. Biomed. Eng. 7*, 55−76.

(20) Algar, W. R., Prasuhn, D. E., Stewart, M. H., Jennings, T. L., Blanco-Canosa, J. B., Dawson, P. E., and Medintz, I. L. (2011) The

controlled display of biomolecules on nanoparticles: a challenge suited to bioorthogonal chemistry. *Bioconjugate Chem. 22*, 825−858.
(21) Liu, W., Howarth, M., Greytak, A. B., Zheng, Y., Nocera, D. G., Ting, A. Y., and Bawendi, M. G. (2008) Compact biocompatible quantum dots functionalized for cellular imaging. *J. Am. Chem. Soc. 130*, 1274−1284.
(22) Sperling, R. A., and Parak, W. J. (2010) Surface modification, functionalization and bioconjugation of colloidal inorganic nanoparticles. *Philos. Trans. R. Soc., A 368*, 1333−1383.
(23) Roullier, V., Clarke, S., You, C., Pinaud, F., Gouzer, G. G., Schaible, D., Marchi-Artzner, V., Piehler, J., and Dahan, M. (2009) High-affinity labeling and tracking of individual histidine-tagged proteins in live cells using Ni2+ tris-nitrilotriacetic acid quantum dot conjugates. *Nano Lett. 9*, 1228−1234.
(24) Lisse, D., Wilkens, V., You, C., Busch, K., and Piehler, J. (2011) Selective targeting of fluorescent nanoparticles to proteins inside live cells. *Angew. Chem., Int. Ed. 50*, 9352−9355.
(25) Mattoussi, H., Palui, G., and Na, H. B. (2012) Luminescent quantum dots as platforms for probing in vitro and in vivo biological processes. *Adv. Drug Delivery Rev. 64*, 138−166.
(26) Howarth, M., Liu, W., Puthenveetil, S., Zheng, Y., Marshall, L. F., Schmidt, M. M., Wittrup, K. D., Bawendi, M. G., and Ting, A. Y. (2008) Monovalent, reduced-size quantum dots for imaging receptors on living cells. *Nat. Methods 5*, 397−399.
(27) Clarke, S., Pinaud, F., Beutel, O., You, C., Piehler, J., and Dahan, M. (2010) Covalent monofunctionalization of peptide-coated quantum dots for single-molecule assays. *Nano Lett 10*, 2147−2154.
(28) Clarke, S., Tamang, S., Reiss, P., and Dahan, M. (2011) A simple and general route for monofunctionalization of fluorescent and magnetic nanoparticles using peptides. *Nanotechnology 22*, 175103.
(29) Sperling, R. A., Pellegrino, T., Li, J. K., Chang, W. H., and Parak, W. J. (2006) Electrophoretic separation of nanoparticles with a discrete number of functional groups. *Adv. Funct. Mater. 16*, 943−948.
(30) Claridge, S. A., Liang, H. W., Basu, S. R., Frechet, J. M. J., and Alivisatos, A. P. (2008) Isolation of discrete nanoparticle-DNA conjugates for plasmonic applications. *Nano Lett. 8*, 1202−1206.
(31) Lin, C. A., Sperling, R. A., Li, J. K., Yang, T. Y., Li, P. Y., Zanella, M., Chang, W. H., and Parak, W. J. (2008) Design of an amphiphilic polymer for nanoparticle coating and functionalization. *Small 4*, 334−341.
(32) Levy, R., Wang, Z., Duchesne, L., Doty, R. C., Cooper, A. I., Brust, M., and Fernig, D. G. (2006) A generic approach to monofunctionalized protein-like gold nanoparticles based on immobilized metal ion affinity chromatography. *ChemBioChem 7*, 592−594.
(33) You, C., Wilmes, S., Beutel, O., Lochte, S., Podoplelowa, Y., Roder, F., Richter, C., Seine, T., Schaible, D., Uze, G., Clarke, S., Pinaud, F., Dahan, M., and Piehler, J. (2010) Self-controlled monofunctionalization of quantum dots for multiplexed protein tracking in live cells. *Angew. Chem., Int. Ed. 49*, 4108−4112.
(34) Howarth, M., Chinnapen, D. J., Gerrow, K., Dorrestein, P. C., Grandy, M. R., Kelleher, N. L., El-Husseini, A., and Ting, A. Y. (2006) A monovalent streptavidin with a single femtomolar biotin binding site. *Nat. Methods 3*, 267−273.
(35) Lata, S., and Piehler, J. (2005) Stable and functional immobilization of histidine-tagged proteins via multivalent chelator headgroups on a molecular poly(ethylene glycol) brush. *Anal. Chem. 77*, 1096−1105.
(36) Gavutis, M., Jaks, E., Lamken, P., and Piehler, J. (2006) Determination of the two-dimensional interaction rate constants of a cytokine receptor complex. *Biophys. J. 90*, 3345−3355.
(37) Cohen, B., Novick, D., Barak, S., and Rubinstein, M. (1995) Ligand-induced association of the type I interferon receptor components. *Mol. Cell. Biol. 15*, 4208−4214.
(38) Appelhans, T., Richter, C. P., Wilkens, V., Hess, S. T., Piehler, J., and Busch, K. B. (2012) Nanoscale organization of mitochondrial microcompartments revealed by combining tracking and localization microscopy. *Nano Lett 12*, 610−616.
(39) Lamken, P., Lata, S., Gavutis, M., and Piehler, J. (2004) Ligand-induced assembling of the type I interferon receptor on supported lipid bilayers. *J. Mol. Biol. 341*, 303−318.
(40) Piehler, J., Thomas, C., Christopher Garcia, K., and Schreiber, G. (2012) Structural and dynamic determinants of type I interferon receptor assembly and their functional interpretation. *Immunol. Rev. 250*, 317−334.